



Intercomparisons of Tracker v1.1 and four other ocean particle-tracking software packages in the Regional Ocean Modeling System

Jilian Xiong and Parker MacCready

School of Oceanography, University of Washington, Seattle, WA 98195, USA

Correspondence: Jilian Xiong (xiongjilian@gmail.com, jxiong7@uw.edu)

Received: 3 March 2023 – Discussion started: 22 May 2023

Revised: 12 January 2024 – Accepted: 11 March 2024 – Published: 29 April 2024

Abstract. Particle tracking is widely utilized to study transport features in a range of physical, chemical, and biological processes in oceanography. In this study, a new offline particle-tracking package, Tracker v1.1, is introduced, and its performance is evaluated in comparison to an online Eulerian dye, one online particle-tracking software package, and three offline particle-tracking software packages in a small, high-resolution model domain and a large coarser model domain. It was found that both particle and dye approaches give similar results across different model resolutions and domains when they were tracking the same water mass, as indicated by similar mean advection pathways and spatial distributions of dye and particles. The flexibility of offline particle tracking and its similarity against online dye and online particle tracking make it a useful tool to complement existing ocean circulation models. The new Tracker was shown to be a reliable particle-tracking package to complement the Regional Ocean Modeling System (ROMS) with the advantages of platform independence and speed improvements, especially in large model domains achieved by the nearest-neighbor search algorithm. Lastly, trade-offs of computational efficiency, modifiability, and ease of use that can influence the choice of which package to use are explored. The main value of the present study is that the different particle and dye tracking codes were all run on the same model output or within the model that generated the output. This allows some measure of intercomparison between the different tracking schemes, and we conclude that all choices that make each tracking package unique do not necessarily lead to very different results.

1 Introduction

Lagrangian particle tracking is a very common and useful tool, especially in the post-processing of existing oceanographic model runs (van Sebille et al., 2018), and is of great value in applied oceanography like pollutant dispersion (e.g., Havens et al., 2009; Nepstad et al., 2022), oil spills (e.g., Nordam et al., 2019), harmful algal blooms (e.g., Giddings et al., 2014; Rowe et al., 2016; Xiong et al., 2023), planktonic larvae (e.g., Brasseale et al., 2019; Garwood et al., 2022), marine plastics (e.g., Onink et al., 2021), and search-and-rescue operations (e.g., Chen et al., 2012). Particle trajectories can be computed “online” along with the velocity fields at every time step as a part of ocean circulation models: for instance, the built-in particle-tracking module “floats” in the Regional Ocean Modeling System (ROMS, Shchepetkin and McWilliams, 2005; Melsom et al., 2022; Aijaz et al., 2024). The trajectories can also be computed “offline” using stored hydrodynamic model output (Dagestad et al., 2018). Generally, offline tracking is more frequently applied in the literature than online tracking given its flexibility, for example, in working with different precalculated velocity fields, testing particle seeding strategies, and particle behaviors (Dagestad et al., 2018; Nordam and Duran, 2020; Hunter et al., 2022).

Many offline particle-tracking software packages have been developed for multiple applications in oceanography, e.g., OceanParcels (Lange and van Sebille, 2017), Ichthyop (Lett et al., 2008), TRACMASS (Döös et al., 2013), PaTATO (Fredj et al., 2016), TrackMPD (Jalon-Rojas et al., 2019), OceanTracker (Vennell et al., 2021), Deft3D-PART (Deltares, 2022), Ariane (Blanke and Raynaud, 1997), and CMS (Paris et al., 2013). Several previous studies have com-

pared one Lagrangian particle-tracking model with passive Eulerian dye experiments to evaluate how well the particle trajectories integrated in a Lagrangian framework can represent the dye spreading in an Eulerian framework (e.g., North et al., 2006; Wagner et al., 2019; Melsom et al., 2022; Nepstad et al., 2022). Yet few (e.g., Daher et al., 2020) have compared different particle-tracking models since the tracking codes are often developed to work with separate ocean models or forcing file formats. It is challenging to draw conclusions by comparing the output from each of them. Given the increasing popularity of particle-tracking techniques in studying ocean transport features, it is useful to evaluate the performance (e.g., its similarity to Eulerian dye transport and computation speed) of the popular particle-tracking software packages that can be assessed in a uniform testbed, e.g., using the same ocean circulation model. Here, we utilized a realistic circulation model, LiveOcean (MacCready et al., 2021), to evaluate several publicly available and commonly used particle-tracking software packages.

LiveOcean is built using ROMS and is a realistic numerical model of ocean circulation and biogeochemistry for the coastal and estuarine waters of the northern California Current System (MacCready et al., 2021). The model is run quasi-operationally, making 3 d forecasts of currents and other water properties every day. It is widely used by a variety of stakeholders concerned with the effects of ocean acidification, hypoxia, harmful algal blooms, and larval transport on fisheries. The model configuration of LiveOcean evolved from many years of research and modeling work in the coastal waters of Oregon, Washington, and most of Vancouver Island and in the Salish Sea (Sutherland et al., 2011; Davis et al., 2014; Giddings et al., 2014; Siedlecki et al., 2015). More details of model setup and validation are given in the Supplement of MacCready et al. (2021). LiveOcean has an offline particle-tracking code written in Python named “Tracker” (v1.1), which has been used to identify the source of estuarine inflow from continental shelves (Brasseale and MacCready, 2021) and track trajectories of the harmful species *Pseudo-nitzschia* in daily post-processing to assist resource managers to decide to open or close Washington beaches for razor clam harvest in combination with beach sampling (Stone et al., 2022). A snapshot of particle trajectories in the daily forecast of LiveOcean on 12 January 2024 can be found in the Supplement of the present study.

To further evaluate the performance of Tracker and conduct multiple particle-tracking model evaluations, three offline tracking codes – LTRANS (Schlag and North, 2012), OpenDrift (Dagestad et al., 2018), and Particulator (Banas et al., 2009) – were selected among other particle codes. We selected these three packages because they all can operate in the original velocity fields solved on an Arakawa “C” grid (Arakawa and Lamb, 1977) used by ROMS, facilitating direct intercomparison without the need for re-gridding velocity. They span a representative range of common programming languages (i.e., Fortran, Python, and MATLAB) as well

as a range of algorithm choices (Table 1). Besides intercomparisons among these offline particle-tracking codes, online passive dye experiments are used as a benchmark to evaluate their performance. The ROMS online particle-tracking module, “floats”, is also tested to supplement the comparisons. To facilitate the implementation of online dye and particle tracking, a new nested hydrodynamic model that only covers the domain of Hood Canal (Fig. 1b) was established using ROMS. The Hood Canal model has a uniform horizontal resolution of 200 m and shares the same 30 vertical layers with LiveOcean. The northern open boundary is interpolated from the LiveOcean large domain, while all other forcings (river and atmospheric forcings) come from the same sources as LiveOcean. Freshwater discharge from an additional eight tiny rivers (Fig. 1b) was added to improve the simulated salinity field in Hood Canal.

In this short paper, we made a series of tests of five total (four offline and one online) particle-tracking software packages to evaluate to what extent they all produce the same answer and to what extent they can reproduce results consistent with a passive dye. The main purpose of this study is to conduct the intercomparisons of some commonly used particle-tracking codes in the same numerical simulations to explore the net effect of the many slightly different choices made by the different developers. The other three offline tracking codes have been rigorously tested by their developers, and we present our own tests of vertical mixing for Tracker. When choosing a particle-tracking code to use, modelers have many considerations. Will the code be easy to use with their model output? Will they be able to modify the code for their specific needs, e.g., introducing vertical particle behavior? Will it run fast enough? Finally, a modeler should have some confidence that regardless of which code they choose the results will be reasonably similar for all the choices. The goal of this intercomparison is primarily to address this final issue of confidence. We also kept track of the computational efficiency and discussed the ease of use of all tracking codes to provide practical guidance about tradeoffs for other researchers.

2 Methods

2.1 Tracker

Tracker is an open-source Python-based Lagrangian particle package designed to work with ROMS hydrodynamic outputs. In addition to the Python standard library, other packages utilized include SciPy (Virtanen et al., 2020), NumPy (Harris et al., 2020), Xarray (Hoyer and Hamman, 2017), and pandas (McKinney, 2010). Random displacement (as a modified random walk) is implemented in the vertical to represent the effects of turbulent mixing and prevent particles from unrealistically accumulating in low-diffusivity areas (Visser, 1997; North et al., 2006; Banas et al., 2009). The horizontal

Table 1. Configurations for different particle-tracking codes.

	Tracker	OpenDrift	Particulator	LTRANS	ROMS online floats
Programming language	Python	Python	MATLAB	Fortran	Fortran
Time step	Self-defined	Self-defined	Self-defined	Self-defined	Same as baroclinic time step
Vertical turbulence	Random displacement	Random displacement	Random displacement	Random displacement	Random displacement
Land boundary	Move particles on land to the middle of the nearest wet rho point	<ul style="list-style-type: none"> – Stranding: particles deactivated – Previous: particles moving back to previous locations – None: particles not interacting with land 	By default, particles carried within one grid cell of land will wait there until flow can carry them away	Particles reflected off the land boundary with an angle the same as the approach angle. The reflect distance equals the distance that particles exceeded the boundary	Particles avoid crossing land boundary
Open boundary	Not specified, remove particles outside boundary in post-processing	Particles deactivated outside the domain (or absorbing boundary)	Particle stops if it will be transported outside the domain in the next time step and wait there until flow moves it around inside the domain	<ul style="list-style-type: none"> – Reflective boundary: treated the same way as land boundary – Sticking boundary: stop moving 	Particles outside open boundary are deactivated
Vertical boundary	Reflect vertically back into the domain by a distance that the particle exceeds the boundary or enforce limits on reflection with the NumPy remainder function if the vertical advection moves particles more than the total water depth	<ul style="list-style-type: none"> – Bottom boundary: lift_to_seafloor, deactivate, previous, or resuspended – Surface boundary: reflective or stick to surface 	Particles move outside the surface (or bottom) will be put back in $\sigma = 0$ (or -1)	Reflect vertically back to the domain with the same distance that particles exceed the boundary	<ul style="list-style-type: none"> – <code>ifdef float_sticky</code>: floats that hit the surface are reflected; floats that hit the bottom get stuck – <code>undef float_sticky</code>: floats that hit the surface or bottom are reflected
Advection scheme	Fourth-order Runge–Kutta	Euler, Second-order Runge–Kutta, fourth-order Runge–Kutta	Second-order Runge–Kutta	Fourth-order Runge–Kutta	Fourth-order Milne predictor and fourth-order Hamming corrector
Interpolation scheme	Nearest neighbor	Bilinear	Bilinear	Water-column profile scheme for 3D and bilinear for 2D variables	<ul style="list-style-type: none"> – Inside masked cells: linear and nearest neighbor – Outside masked cells: bilinear
Backward tracking	Able to include	Yes	Able to include	Yes	Not able to do backtracking
Ease of use	<ul style="list-style-type: none"> – Read ROMS history file – No compilation required, easy to set up Python environment – Flexible to define the initial particle release location and add user-defined functions – Running platform independent 	<ul style="list-style-type: none"> – Need to concatenate grid information to ROMS history file – No compilation required, easy to set up Python environment – Flexible to define the initial particle release location, modify existing modules, and write user-defined modules – Running platform independent 	<ul style="list-style-type: none"> – Read ROMS history file – No compilation required but MATLAB is a commercial software – Flexible to define the initial particle release location – Running platform independent 	<ul style="list-style-type: none"> – Read ROMS history file but each file must have at least three time steps – Take time to compile source code – Flexible to define the initial particle release location – Run on Linux machines – Require a long time run for large number of particles 	<ul style="list-style-type: none"> – Require experience to compile ROMS source code and set up HPC environment – The initial particle release location seems to be not very handy/flexible to specify – Run on Linux machines in parallel mode
Source code	https://github.com/parkermac/LO/tree/v1.1/tracker (last access: 20 April 2024)	https://opendrift.github.io/ (last access: 20 April 2024)	https://github.com/neilbanas/particulator (last access: 20 April 2024)	https://northweb.hpl.umces.edu/LTRANS.htm (last access: 20 April 2024)	https://www.myroms.org/wiki/floats.in (last access: 20 April 2024)

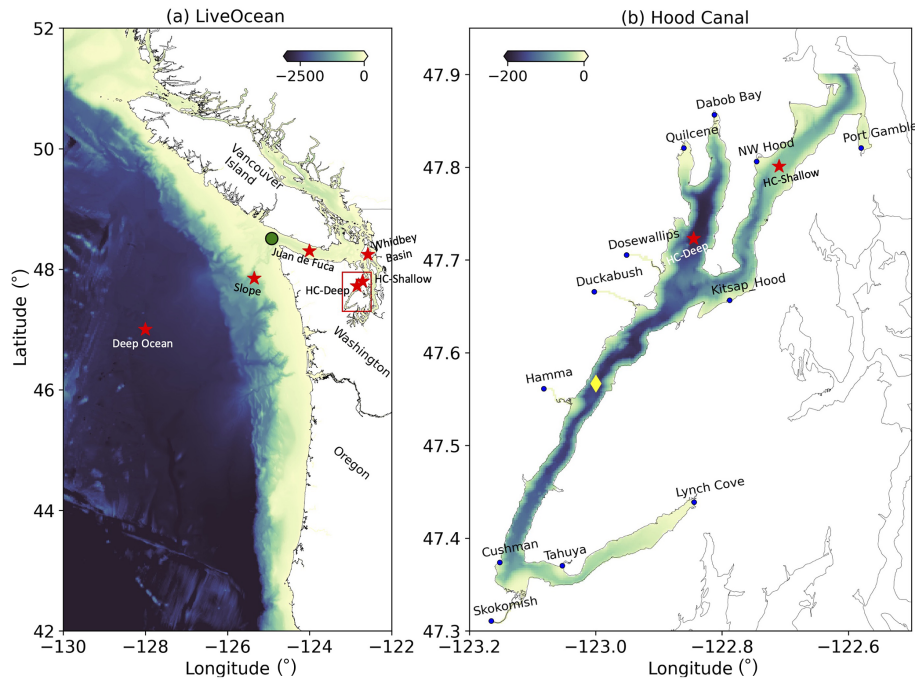


Figure 1. (a) LiveOcean and (b) Hood Canal model domains and bathymetry. In panel (a), the red stars represent sites selected for one-dimensional vertical well-mixed condition tests. The green dot indicates the particle release location to test offline particle-tracking codes in the LiveOcean domain. In panel (b), the yellow diamond indicates particle and dye release location using the Hood Canal model domain. The blue dots represent locations with river inputs.

and vertical transport of particles are calculated as

$$x_{n+1} = x_n + u \cdot \Delta t, \quad (1)$$

$$y_{n+1} = y_n + v \cdot \Delta t, \quad (2)$$

$$z_{n+1} = z_n + \left(w + \frac{\partial AK_s}{\partial z} \right) \cdot \Delta t + R \sqrt{2AK_s} \cdot \Delta t, \quad (3)$$

where x_n , y_n , and z_n are the horizontal and vertical particle positions (in meters) at time step n after the advection, Δt is the time step, and R is a normally distributed random function with a mean of 0 and a standard deviation of 1. AK_s is the vertical diffusivity evaluated at $(z_n + 0.5 \frac{\partial AK_s}{\partial z} \Delta t)$, and the derivative $\frac{\partial AK_s}{\partial z}$ is evaluated at z_n (North et al., 2006). Before calculating the vertical derivatives, the vertical profile of eddy diffusivity AK_s is smoothed using a three-point Hanning window (Thomson and Emery, 2014) to reduce the potential sharp gradient in vertical diffusivity that could cause particle aggregations, following the four-point and eight-point moving average used in North et al. (2006). Specifically, $AK_s [1 : -1] = 0.25 \times AK_s [0 : -2] + 0.5 \times AK_s [1 : -1] + 0.25 \times AK_s [2 : -1]$. The index follows rules in Python. In addition, the surface AK_s and bottom AK_s are adjusted to be equal to the values one grid point in. The choice was motivated by the fact that we used a nearest-neighbor search algorithm and were concerned that particles close to the top or bottom might use a near-zero diffusivity. A fourth-order Runge–Kutta integration scheme was

used in Eqs. (1)–(3) to displace particles from the current location to the next location after an internal time step of Δt . $\Delta t \ll \min(1/AK_s'')$, where AK_s'' is the second derivative of the vertical diffusivity, is required to satisfy the vertical random displacement model criterion (Visser, 1997). The time step for both horizontal and vertical particle tracking was set at 300 s after examining the vertical profiles of AK_s'' at six sites (used for the well-mixed condition test in Sect. 2.1.1) from deep open ocean to the inner Salish Sea.

To speed computation, Tracker uses pre-computed nearest-neighbor search trees to find velocities (u , v , w in Eqs. 1–3) and other fields (e.g., diffusivity, temperature, and salinity) used for moving each particle forward. The accuracy of Lagrangian particle trajectory calculated with different numerical integrators and interpolation methods was discussed in Nordam and Duran (2020). In our development experiments, we found that the combination of nearest-neighbor interpolation and fourth-order Runge–Kutta integrator can speed computation for the large grid size of the model domain and ensure the accuracy of particle trajectory in regions with complex shoreline geometries, e.g., the curving channels in the Tacoma Narrow in the southern Salish Sea. The initial particle locations are seeded in the coordinate of longitude and latitude (an example can be found in the `get_ic` function in `experiments.py` in the Supplement). The horizontal advection (in meters) of particles is converted to degrees using an Earth radius calculated based on the local latitude

(earth_rad function was given in zfun.py in the Supplement) and the particle locations (long, lat) are saved in the format of NetCDF. For the land boundary, if a particle is advected onto land, it will be moved to a neighboring grid cell with a random direction. The numerical model does not resolve every process in the nearshore region (waves, rip currents, etc.); therefore, this is a practical way to make sure that particles do not get caught in the boundaries or in corners. To test if Tracker can give trustworthy results, one important test is the preservation of vertical well-mixed conditions (North et al., 2006). Another is the similarity to dispersion of an inert dye.

2.1.1 Well-mixed condition test

Using the hourly saved hydrodynamic output from LiveOcean, six sites in different dynamic settings from the deep ocean to the Salish Sea (Fig. 1a) were selected to perform the well-mixed condition (WMC) tests on Tracker with horizontal and vertical advection turned off and a random displacement model implemented in the z direction (i.e., the particle location is only controlled by $z_{n+1} = z_n + \frac{\partial AK_s}{\partial z} \cdot \Delta t + R\sqrt{2AK_s \cdot \Delta t}$). For each site, 4000 particles were seeded uniformly from the free surface to the bottom. The WMC tests were run for 12 h with both a time-dependent diffusivity profile (on 1 January 2021 from 00:00:00 to 12:00:00) and a steady diffusivity profile (on 1 January 2021 at 00:00:00, Fig. 2). The time step for tracking particles in WMC tests is 300 s. To satisfy the WMC test, the initially well-mixed particles are expected to remain uniform in a statistical sense regardless of the diffusivity profiles, consistent with the Eulerian solution to the one-dimensional vertical diffusion equation ($\frac{\partial C}{\partial t} - \frac{\partial}{\partial z} \left(K \frac{\partial C}{\partial z} \right) = 0$, where K is eddy diffusivity), with an initial uniform concentration, $C(z) = C_0$, and no flux boundaries, $K \frac{\partial C}{\partial z} = 0$ (Visser, 1997; Rowe et al., 2016; Nordam et al., 2019). Metrics of success for WMC tests follow North et al. (2006) so that particle numbers were compared to a “non-significant range” to test whether the WMC was satisfied. To obtain the non-significant range (dashed lines in Fig. 2), 4000 snapshots of 4000 randomly distributed particles were generated and the number of particles was then calculated in 28 evenly spaced intervals. The mean values of the highest (187.3) and lowest (102.5) values of particle numbers at each interval from the 4000 snapshots were used to define the upper and lower limit of the non-significant range (North et al., 2006).

2.2 Other offline particle-tracking software packages

Here, we briefly describe the three other offline particle-tracking packages – LTRANS (North et al., 2006), Particulator (Banas et al., 2009), and OpenDrift (Dagestad et al., 2018) – with more details about their configurations given in Table 1 and provided in the respective references.

LTRANS is a well-documented tool written in Fortran 90, specifically for output from ROMS. It has broad applications

in studying larvae transport (North et al., 2008), oil spills (North et al., 2011; Testa et al., 2016), coastal connectivity (Li et al., 2014), plastics (Liang et al., 2021), algae (Wang et al., 2022), etc. Particulator is written in MATLAB, mostly specific to output from ROMS, and has been used to study water pathways (Banas et al., 2015; Stone et al., 2018) and harmful algal blooms (Giddings et al., 2014). OpenDrift is written in Python and has flexibility to work with forcing data from different ocean models, including ROMS. It has rather wide-ranging applications in tracking particles with diverse properties, e.g., fish eggs (Melsom et al., 2022), Environmental DNA (Andruszkiewicz et al., 2019), oil, chemical tracers, sediment, capsized boats, and icebergs (Dagestad et al., 2018). Given the different interpolation schemes, numerical integrators, and how turbulent dispersion and encounters with model boundaries are treated, we limit our inter-model comparisons by only considering advection of passive (or neutrally buoyant) particles by the three-dimensional flow and vertical turbulent mixing (without surface windage and waves).

2.3 Online passive dye experiment and particle tracking

A passive dye experiment was conducted to determine if the particle-tracking model predictions agree with simulated diffusion. Dye can be considered the “truth” that particle-tracking codes seek to replicate. However, this idea is complicated by the presence of numerical mixing which is intrinsic to model advection algorithms (Burchard and Rennau, 2008; Ralston et al., 2017). Numerical mixing, defined by the decrease in tracer variance due to discretization errors in the tracer advection scheme, increases the dispersion of tracers (Ralston et al., 2017). In Broatch and MacCready (2022), numerical mixing was found to account for one-third of the total mixing of salinity in the LiveOcean model inside the Salish Sea. While most model studies do not quantify numerical mixing, those that have, mostly limited to estuaries, show that it is significant. Thus, we expect in general that dye will experience greater horizontal and vertical dispersion than particles, especially in regions with strong horizontal gradients.

Using the Hood Canal model, a passive dye was introduced from a grid cell in the middle of the water column of the channel (Fig. 1b) and was tracked for 7 d starting from 1 June 2021 at 00:00:00. Before activating the dye module, the hydrodynamic simulations were run for the whole year of 2021 with daily saved restart files. An additional variable, “dye_01”, was added to the restart file on 1 June 2021 at 00:00:00 with a concentration of 1 in the selected grid cell and 0 elsewhere. The time step for dye transport is 40 s. The MPDATA advection scheme (Smolarkiewicz, 1984) was applied for dye, the same as temperature and salinity. This scheme effectively reduces numerical dispersion and prevents negative concentration values (Melsom et al., 2022).

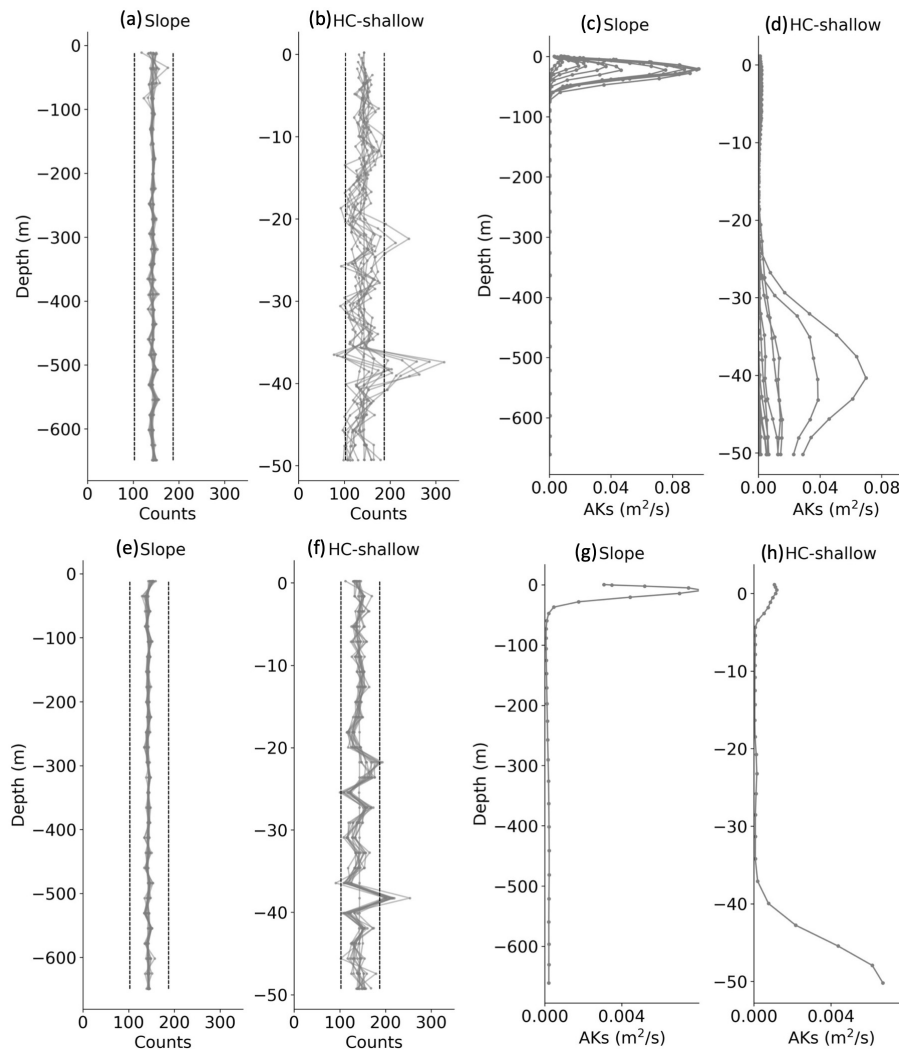


Figure 2. One-dimensional vertical well-mixed condition (WMC) tests at two sites (Fig. 1a) in the LiveOcean model domain and the associated profiles of vertical diffusivity (c–d, g–h). (a–b) WMC tests using time-dependent diffusivity profiles shown in panels (c)–(d). (e–f) WMC tests using steady diffusivity profiles in panels (g)–(h). All WMC tests were conducted for 12 h with hourly output and a time step of 300 s. The dashed lines in panels (a)–(b) and (e)–(f) indicate the non-significant range, outside of which the WMC tests fail.

To compare Eulerian dye and Lagrangian particles, 10^5 particles with a distribution of $100 \times 100 \times 10$ (longitude \times latitude \times vertical) were released from the same model grid cell at the same time as dye release for all four offline tracking codes. Particle tracking was driven by the hourly saved history files in each case. Each particle was associated with a particular mass ε_0 obtained as the ratio of the initial dye mass to the total particle number (i.e., 10^5). The time step for offline particle tracking is 300 s. Previous experiments with Tracker showed this time step was required in LiveOcean in regions with strong currents and complex channel shape. Longer time steps would sometimes advect particles over narrow land regions instead of following curving channels. A slightly different seeding strategy was applied for the ROMS online particle module for convenience.

The 10^5 particles were distributed uniformly along the diagonal of the selected model grid cell, which gives the same initial centers of mass for particles in x , y , and z dimensions. The thickness of the selected model grid cell is about 5 % of the total local depth, and the adjusted particle initialization in ROMS online tracking is expected not to significantly influence the intercomparisons. The time step for online tracking is 40 s. Additional comparisons for the four offline particle packages were conducted using the large LiveOcean model domain and its hourly saved history file. Within a $1 \text{ km} \times 1 \text{ km}$ square at the free surface and in the middle water column near the mouth of the strait of Juan de Fuca, 10^4 particles were evenly distributed (Fig. 1a). Particles were tracked for 7 d from 1 January 2021 at 00:00:00 with a time step of 300 s. In all experiments mentioned above, dye con-

centration and particle trajectory positions were saved hourly for further analysis.

To compare the mean pathways of dye and particles, their centers of mass were calculated as

$$M_{x_dye}(t) = \frac{\sum_{i=1}^{N_{total_grid}} x_{i_dye} \cdot C_{i_dye} \cdot V_i}{\sum_i C_{i_dye} \cdot V_i}, \quad (4)$$

$$M_{x_particle}(t) = \frac{\sum_{i=1}^{N_{total_particle}} x_{i_particle}}{N_{total_particle}}, \quad (5)$$

where N_{total_grid} is the total number of model grid cells, $N_{total_particle}$ is the total particle number, C_{i_dye} is the dye concentration in model grid cell i , and V_i is the corresponding grid cell volume. The centers of mass in the y and z dimensions were calculated with similar equations.

3 Results and discussion

3.1 Well-mixed condition tests

The vertical particle distributions from WMC tests for Tracker are shown in Fig. 2. Results at other locations (not shown) gave similar results. The site with deeper depth passed WMC tests for both time-dependent and steady vertical diffusivity profiles. Occasional failures of WMC tests were found at the shallow site, specifically the vertical regions with low diffusivity and increasing gradient. Particles tend to cluster in low-diffusivity regions, e.g., ~ 38 m at the Hood Canal site (HC-shallow site in Fig. 2b, f). Previous studies suggested that demonstration of WMC was influenced by discontinuities in AK_s profiles, the interpolation scheme used to estimate AK_s and its vertical gradient, and the time step of particle tracking (Brickman and Smith, 2002; North et al., 2006). Here, we demonstrated that the three-point Hanning window used to smooth AK_s profiles, the nearest-neighbor interpolation scheme used to obtain AK_s , and a time step of 300 s in Tracker generally pass the WMC test for sites from offshore deeper than 2500 m to the Salish Sea shallower than 40 m; however, there are occasional failures. We proceed by assuming that the effects of such failures would, in practice, be smeared out as particles are moved rapidly by tidal advection through a wide range of conditions.

3.2 Comparisons among particle-tracking software packages using the Hood Canal model

3.2.1 Offline versus online particle tracking

Centers of mass of trajectories from all particle-tracking codes, relative to the initial release location, are shown in Fig. 3. Particles were initialized at the low tide, and the tracking was followed by a flood tidal phase. A relatively good inter-model match was achieved for the first 5–6 h during the flood tide. After this point, all models still tend to follow the

same trend but drift apart presumably because of these different interpolation and advection schemes and online or offline tracking. The differences increase with time since different particle locations sample different velocities and diffusivities.

Horizontal spreading of vertically integrated particle mass (Fig. 4) and vertical distributions of particles (Fig. 5) exhibit similar but not equivalent evolutions among all tracking codes. Particles from OpenDrift tend to show less spread. Generally, results from online tracking stays in the middle of other offline tracking codes. Compared to offline tracking, online particle trajectory is updated every time step along with the hydrodynamic model runs and vertical transport is better accounted for (Ricker and Stanev, 2020). However, offline tracking provides more flexibility to incorporate forcings from more than one numerical model or observational database. In offline mode, it is easier to modify algorithms to include user-defined processes (e.g., diel vertical migrations, settling, and resuspension) and test parameters or different particle seeding strategies without rerunning the full ocean model, which can be computationally expensive (Dagestad et al., 2018; Hunter et al., 2022; Melsom et al., 2022). Simulation backward in time is also more easily performed offline. To the best of our knowledge, no studies so far have targeted backward tracking using online particle-tracking models. On the other hand, updating trajectories in offline tracking could suffer from inaccuracies induced by the interpolation scheme since it reads subsampled or averaged model outputs, which could smear out short-time and small-scale advective processes simulated by ocean circulation models (Wagner et al., 2019; Melsom et al., 2022).

3.2.2 Lagrangian particle tracking versus Eulerian passive dye

Using the Eulerian dye model prediction as a benchmark, we evaluate the performance of Lagrangian particle-tracking models. Like the comparisons among different particle-tracking codes, the particle and dye models also agree well with each other within the first few hours following their initial release (Fig. 3). The evolution of the center of mass from online particle tracking matches the best with the center of mass of dye. The horizontal center of mass of dye stays between all particle-tracking models, while dye predicts somewhat deeper mixing than particle models, with the vertical center of mass being about 5–10 m deeper after 30 h (Fig. 3c). Greater vertical spreading of dye was also observed in the histogram (Fig. 5). Dye fills the upper 20–140 m after 2 d while particles are still confined to a depth range of 50–90 m around their release depth. To obtain the histogram of vertical dye distribution, dye mass inside each model grid cell was converted to an equivalent number of particles via the constant ε_0 (defined in Sect. 2.3). The vertical coordinate in the center of the grid cell that contains dye was then used to represent the vertical location of dye-converted particle number.

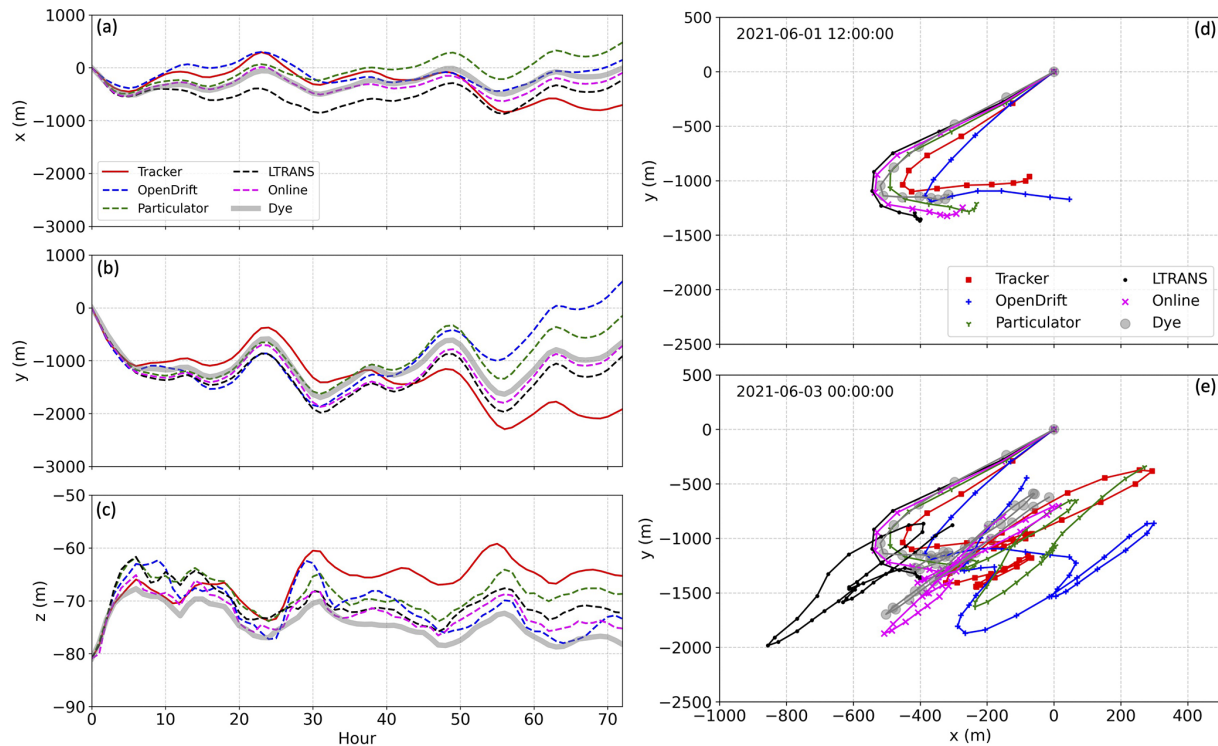


Figure 3. The centers of mass in x , y , and z directions obtained from offline and online particle tracking and passive dye experiments using the Hood Canal model. (a–c) Evolution of the centers of mass. (d–e) The centers of mass in x and y directions with particles tracked for (d) 12 h and (e) 48 h. Particles and dye were released inside Hood Canal on 1 June 2021 at 00:00:00 (Fig. 1b).

This conversion might lead to the spiky vertical distribution in the early stage of dye transport (as seen in Fig. 5a).

The horizontal spread of vertically integrated dye and particle mass is shown in Fig. 4. Generally, dye is also more widespread than particles in the horizontal (similar to patterns observed in, e.g., Melsom et al., 2022, and Nepstad et al., 2022). Low values of dye spread faster than particles and cover a greater area. However, the spread of high mass concentration exhibits a reasonable degree of similarity, indicating that Lagrangian particle-tracking models all yield similar simulations of vertical dispersion, although formulations for particles and dye transport differ largely in details (North et al., 2006). It is suggested (North et al., 2006; Wagner et al., 2019; Broatch and MacCready, 2022; Nepstad et al., 2022) that the vertically reconstituted diffusivity profile, vertical model grid resolution, total particle number, temporal subsampling of velocity fields, and numerical mixing influencing dye concentration give rise to the deviations between particle tracking and inert dye component.

Comparing online particle tracking and online passive dye experiments in ROMS, Lagrangian particle tracking tends to be more computationally demanding (Table 2). The average time for running hydrodynamics for 1 d in the Hood Canal model is about 160 s using 200 cores on a Linux cluster. The running time increases a little to 196 s with the dye module activated, and it increased to 1218 s when the floats module

was activated to track 10^5 particles. However, particle tracking, especially offline tracking, is more flexible, and dye calculations can be more costly in some instances. For example, multiple passive dyes are required to represent multi-component river-borne discharges (e.g., nutrients, pathogens, freshwater) but particles can carry all these properties in one trajectory tracking experiment (Banas et al., 2015). Particle tracking is also economical in disk space since only particle locations and associated water properties (e.g., salinity and temperature) are stored, but dye is usually saved for the whole model domain (Melsom et al., 2022). In addition, particle-tracking models can resolve particle displacement at sub-grid scales (Alosairi et al., 2020; Xiong et al., 2023) because dye is a grid cell property.

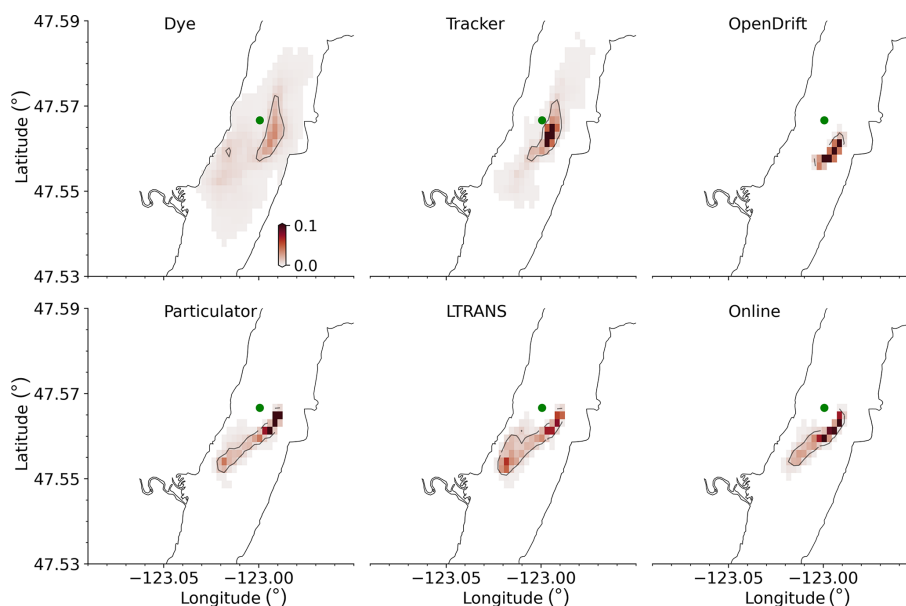
3.3 Comparison among offline particle-tracking software packages using the LiveOcean model

Additional comparisons just among the four offline particle-tracking codes were conducted using the larger LiveOcean model domain. Particles were released from the free surface and the middle water column in the coastal area on 1 January 2021 at 00:00:00 (Fig. 1a) and particle dispersal regions along the coast are with a horizontal grid resolution of ~ 1000 m (Fig. 6d, h). The particle-tracking period was dominated by southerly winds, favorable for northward

Table 2. Computation time (seconds) for ROMS simulations conducted for 1 d. All cases were run on the University of Washington's Hyak supercomputer with 200 cores.

Cases	Average* computation time for 1 d run
Hydrodynamic run	160
Hydrodynamic run + passive dye	196
Hydrodynamic run + online particle tracking (100 000 particles)	1218

* Averaged from 1 to 7 June 2021.

**Figure 4.** Snapshot of vertically integrated dye and particle mass (scaled to 0–1 by the initial dye or particle mass) after 1 d of simulation using the Hood Canal model. The green dot indicates the initial dye and particle release location. The black contour in each panel represents a value of 0.01.

and onshore near-surface currents over the shelf (Giddings et al., 2014). Thus, particles exhibit net northward transport, and the surface-released particles move closer to the coast (Fig. 6h–i). Besides the center of mass, particle density (i.e., a ratio of the vertically integrated particle numbers in each horizontal grid cell to the respective grid cell area) was also calculated (Fig. 7). A relatively good match in the center of mass among these tracking codes is evident for about 1 d of tracking (Fig. 6). This suggests that the decorrelation time (Klocker and Abernathy, 2014) is about 1 d in this region. After that, the centers of mass still follow a similar trend but with increasing separations. Note that Tracker produced a large vertical downward displacement during hours 13–22 (Fig. 6g) in the case of mid-depth release, likely due to the greater vertical velocity and weaker stratification experienced by the center of particle mass. The horizontal center of mass calculated by Tracker is closer to the coastline within this period (Fig. 6h). Generally, the horizontal advection due to different interpolation and integration methods leads particles to different dynamic environments and results in greater

(or less) vertical advection. The spatial coverages of particles in the horizontal and vertical also share similar patterns but exhibit somewhat different local accumulation patches (Figs. 7–8). As we saw in the Hood Canal experiments, all four offline particle-tracking codes have similar performance when they track the same water mass in the coarser model domain and in the shelf environment. Note, however, in Fig. 8 that there are real differences in the details of vertical particle distribution among the models after 2 d. These result in part from the details of the algorithms used for vertical dispersion and from particles experiencing different vertical mixing associated with different horizontal locations.

3.4 Computation time

Although all tested offline particle-tracking codes share similar predictions compared with online particle tracking and online Eulerian dye, especially for the first few days, computation efficiency is another important metric for their performance evaluation. The computation time for each offline

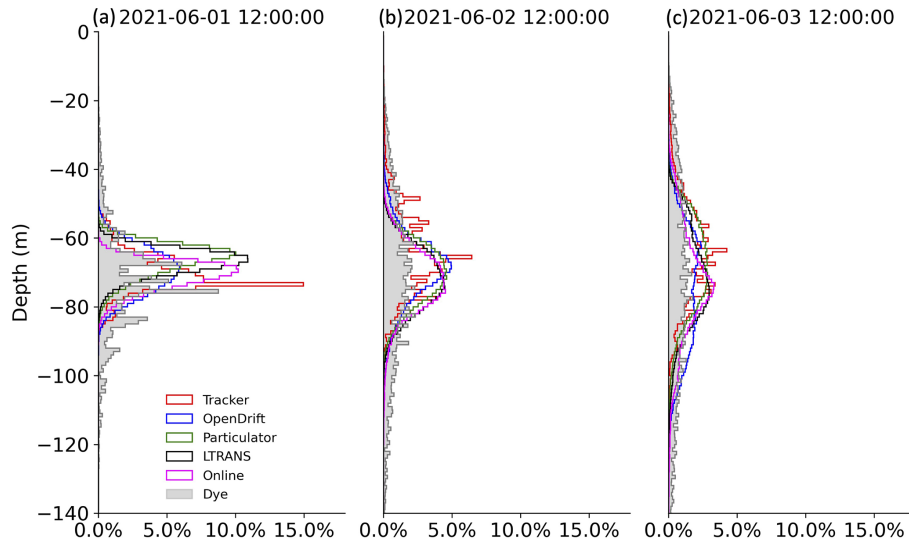


Figure 5. Histogram of vertical particle and dye distributions using Hood Canal model at 12, 36, and 60 h after release. The effects of numerical mixing may be the cause of the greater vertical spread of dye versus particles.

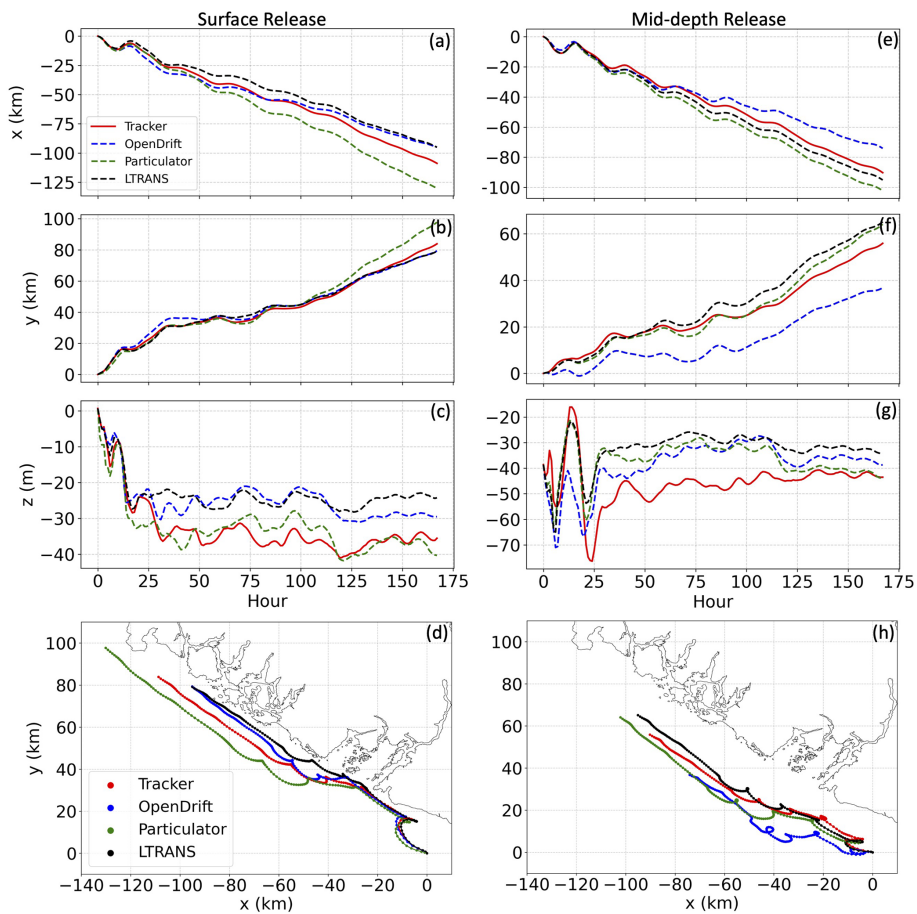


Figure 6. The centers of mass in x , y , and z directions for all four offline particle-tracking codes simulated using hydrodynamic outputs from the LiveOcean model. (a–c) Particles released from the free surface. (e–g) Particles released from the middle water column. (d, h) Centers of mass in x and y directions.

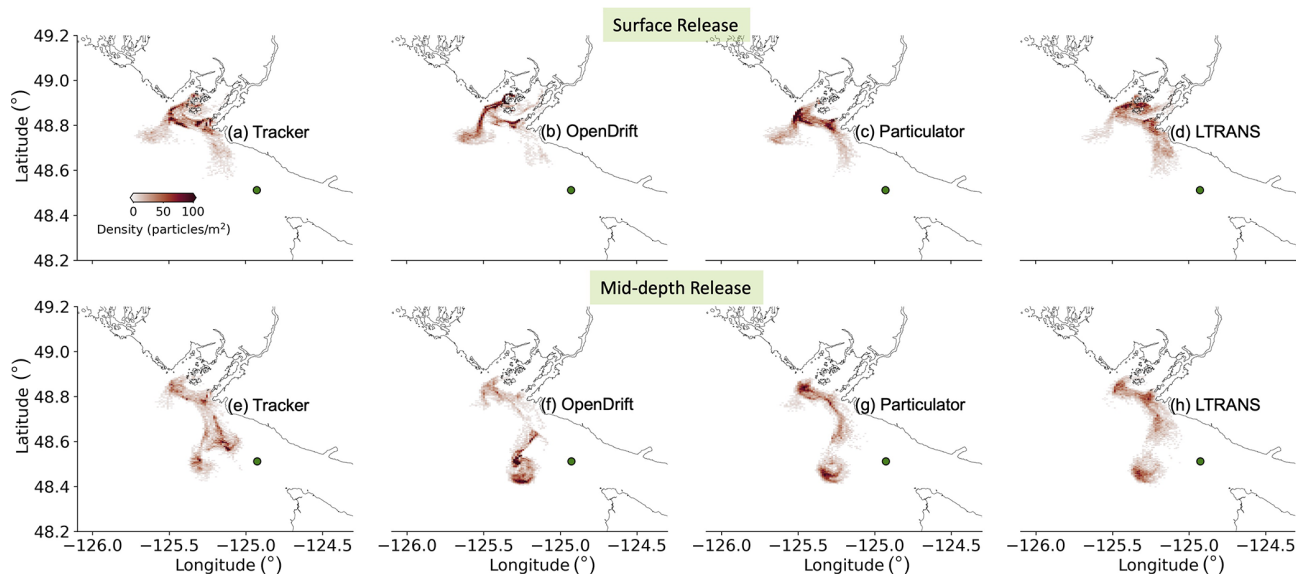


Figure 7. Vertical integral of particle densities for all four offline particle codes after 2 d of tracking using hydrodynamic outputs from the LiveOcean model. **(a–d)** Particles were released from the free surface. **(e–h)** Particles were released from the middle water column. Green dots represent particle release location.

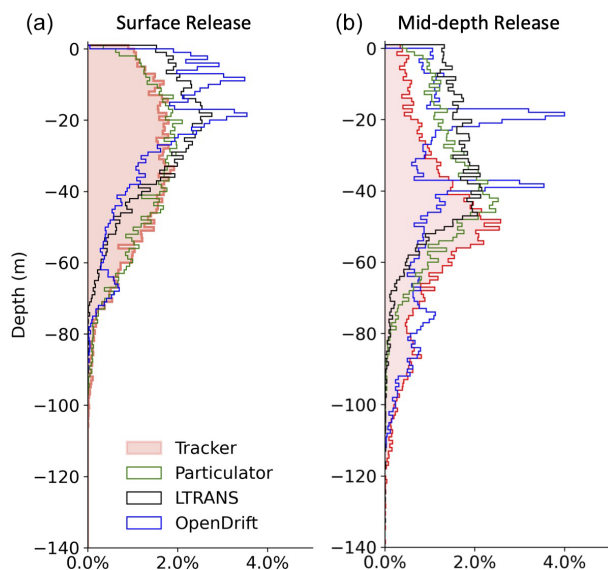


Figure 8. Histogram of vertical particle distribution for all four offline particle codes after 2 d of tracking using hydrodynamic outputs from the LiveOcean model. **(a)** Particles released from the free surface. **(b)** Particles released from the middle water column.

tracking code was recorded using both the small domain of the Hood Canal model and the large domain of the LiveOcean model (Fig. 9; Table 3). Each particle model was run to track neutrally buoyant particles for 25 h with a time step of 300 s. Particle locations, temperature, and salinity at each particle's location were saved hourly. The total particle number varied from 10^0 to 10^6 . The computation time tests were

conducted using an Apple M1 Pro for Particulator and OpenDrift and a Linux machine for LTRANS. We recorded the computation time of Tracker on both the Apple M1 Pro and the Linux machine.

The two tracking codes that were written in Python, Tracker and OpenDrift, had close computation costs when Tracker was tested on the Linux machine and OpenDrift was tested on a laptop (Fig. 9), while the performance of Tracker on the same laptop is faster by a factor of 2–3 compared to that on the Linux machine, perhaps because of different file access speeds between solid-state and RAID drives used to store the model output. The computation time of Tracker and OpenDrift increases with increased particle number, with the largest increase taking place when running 1 million particles. The LTRANS, written in Fortran, runs fast with a small number of particles, but the computation requires a much longer time than other codes with increased particle number and even becomes prohibitive when tracking 1 million particles in the large LiveOcean domain with a grid dimension of $1302 \times 662 \times 30$. Generally, more time is required to track particles in a larger model domain than a smaller one for all offline tracking codes. One interesting finding is that for Particulator, written in MATLAB, the computation time is only weakly influenced by the total particle number and the code can run very fast with the 1 million particles. In the large LiveOcean domain, generally, Tracker requires the least computation time among those tracking packages that were tested on the same laptop; for example, Tracker is 10 times faster than Particulator when the tracking number is less than 10^4 . The interpolation and advection scheme, algorithm structures, and programming languages could all affect

Table 3. Computation time (seconds) for different particle-tracking software packages using the Linux machine or Mac with hydrodynamic outputs saved from a small Hood Canal model domain and a large LiveOcean model domain. All cases were run for 25 h with a time step of 300 s and hourly output with particle locations and temperature/salinity recorded by each particle.

Particle number	Hood Canal model					LiveOcean model				
	Tracker (Linux)	Tracker (Mac)	OpenDrift (Mac)	Particulator (Mac)	LTRANS (Linux)	Tracker (Linux)	Tracker (Mac)	OpenDrift (Mac)	Particulator (Mac)	LTRANS (Linux)
1	16.0	8.5	55.5	87.4	3.5	205.8	67.2	297.2	878.8	92.9
10	29.9	19.6	58.3	87.1	4.5	209.2	77.6	295.8	875.0	95.1
100	44.6	21.0	55.5	86.4	12.0	237.9	79.5	300.7	863.3	118.4
1000	53.8	25.0	63.2	87.3	83.2	236.6	82.5	303.8	883.0	328.7
10 000	129.1	61.5	148.2	103.9	193.5	308.9	121.3	376.1	882.7	2437.3
100 000	701.0	398.0	915.7	118.4	7931.8	1001.9	462.0	1234.0	941.8	23325.7
1 000 000	7093.0	2715.2	8419.8	333.0	/	7309.3	3063.7	7678.2	1208.0	/

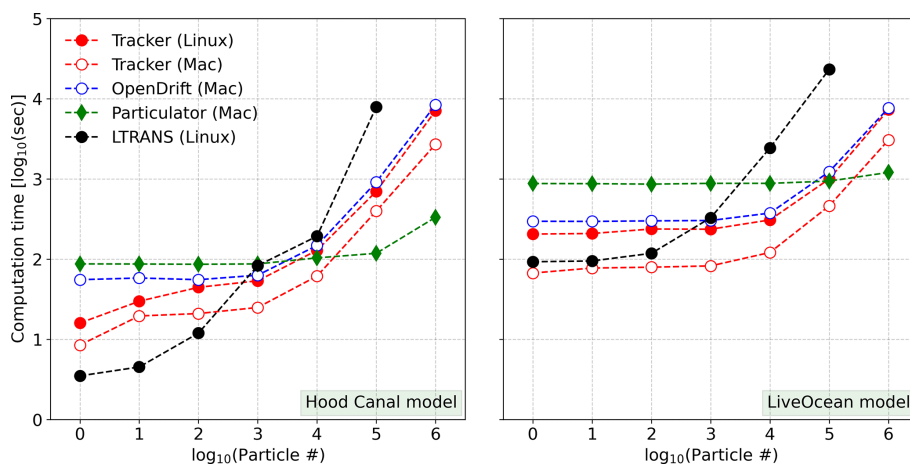


Figure 9. Computation time for tracking particles for 25 h with a time step of 300 s for all four offline particle-tracking codes. The total particle number increases from 10^0 to 10^6 . The computation time for LTRANS was obtained on a Linux machine, while the computation time for Particulator and OpenDrift was obtained on an Apple M1 Pro. Tracker was tested both on a Linux machine and on a Mac. The computation cost for LTRANS with 1 million particles is prohibitive on the Linux machine when testing it with the large LiveOcean domain; for the small Hood Canal domain, the computation time of LTRANS is about 25 h (estimated from the timestamp of the hourly output files that were saved separately).

the computation cost (Table 1). It is beyond the scope of this paper to explore the detailed tradeoffs between these factors, and instead we hope the results of computation time may be one piece of information scientists can use when choosing a particle-tracking package and designing an experiment.

4 Conclusions

In this work, we introduced a new offline Lagrangian particle-tracking model, Tracker v1.1, and tested its ability to preserve vertical well-mixed conditions. We also evaluated its performance compared with online Eulerian dye, one online particle-tracking code, and three offline particle-tracking codes using a high-resolution (200 m grid size) ocean circulation model. Additional comparisons were performed for all four offline tracking codes in a larger model domain

with a horizontal grid resolution of ~ 1000 m in the particle-tracking region.

We show that the mean advection pathways and spatial distributions of dye and particles were reasonably similar when they were tracking the same water mass. The spreading of Eulerian dye is more dispersive with a wider distribution of low concentrations. Similar inter-model comparisons were observed in both small (fine) and large (coarser) model domains. The passive dye was solved in a fixed Eulerian framework that addresses the advection and diffusion equation, which might suffer from spurious numerical mixing. The Lagrangian particle-tracking model employs a movable frame of reference. Online tracking may be expected to give more accurate results because it uses a much shorter time step between velocity fields but lacks flexibility compared to offline tracking. In our experiments, results from on-

line particle tracking were not obviously different from those of any of the offline tracking packages. Although offline tracking is influenced by subsampled model output, parameterization of vertical turbulence mixing, and interpretation scheme, its flexibility and reliability against passive Eulerian dye and online tracking make it a useful and cost-effective tool in tracking transport pathways in oceanography. Finally, the reasonable preservation of well-mixed conditions, speed improvements in large model domains, and similar performance against other particle-tracking codes and passive dye achieved by Tracker suggest that it is a reliable and efficient particle-tracking package to use with ROMS. All tests in this study used a ROMS grid aligned along lines of constant latitude and longitude. In principle, Tracker should work on a more general grid, but this has not been tested.

Code and data availability. All example codes and hydrodynamic fields that were used to test the five particletracking packages in this study are available at <https://doi.org/10.5281/zenodo.10810102> (Xiong and MacCready, 2024).

Supplement. The supplement related to this article is available online at: <https://doi.org/10.5194/gmd-17-3341-2024-supplement>.

Author contributions. PM is the primary developer for Tracker and the LiveOcean model. JX developed the Hood Canal model and carried out all the particle tracking and dye release experiments. JX drafted the manuscript and PM contributed to the review and editing.

Competing interests. The contact author has declared that none of the authors has any competing interests.

Disclaimer. Publisher's note: Copernicus Publications remains neutral with regard to jurisdictional claims made in the text, published maps, institutional affiliations, or any other geographical representation in this paper. While Copernicus Publications makes every effort to include appropriate place names, the final responsibility lies with the authors.

Acknowledgements. We would like to thank David Darr for technical support, Elizabeth Allan for sharing example codes to run OpenDrift, Elias Hunter and Elizabeth North for useful suggestions to run LTRANS, Aurora Leeson for preparing the tiny river discharge data that were included into Hood Canal model domain, Erin Broatch for processing the ORCA buoy data for Hood Canal model calibration, and Dongxiao Yin for useful discussions during the preparation of the manuscript. We also appreciate our topic editor, Ignacio Pisco, one anonymous reviewer, and Tor Nordam for their constructive suggestions and comments on the manuscript.

Financial support. This study is based upon research supported by the Office of Naval Research (award no. N00014-22-1-2719) and also supported by the National Science Foundation (NSF; award no. 2122420) and NOAA (grant no. NA21NOS0120168-T1-01).

Review statement. This paper was edited by Ignacio Pisco and reviewed by Tor Nordam and one anonymous referee.

References

- Aijaz, S., Colberg, F., and Brassington, G. B.: Lagrangian and Eulerian modelling of river plumes in the Great Barrier Reef system, Australia, *Ocean Model.*, 188, 102310, <https://doi.org/10.1016/j.ocemod.2023.102310>, 2024.
- Alosairi, Y., Al-Salem, S. M., and Al Ragum, A.: Three-dimensional numerical modelling of transport, fate and distribution of microplastics in the northwestern Arabian/Persian Gulf, *Mar. Pollut. Bull.*, 161, 111723, <https://doi.org/10.1016/j.marpolbul.2020.111723>, 2020.
- Andruszkiewicz, E. A., Koseff, J. R., Fringer, O. B., Ouellette, N. T., Lowe, A. B., Edwards, C. A., and Boehm, A. B.: Modeling environmental DNA transport in the coastal ocean using Lagrangian particle tracking, *Front. Mar. Sci.*, 6, 477, <https://doi.org/10.3389/fmars.2019.00477>, 2019.
- Arakawa, A. and Lamb, V. R.: Computational design of the basic dynamical processes of the UCLA general circulation model, edited by: Arakawa, A. and Lamb, V. R., in: *General circulation models of the atmosphere, methods in computational physics: Advances in research and application*, vol. 17, 173–265, Elsevier, Amsterdam, <https://doi.org/10.1016/B978-0-12-460817-7.50009-4>, 1977.
- Banas, N. S., MacCready, P., and Hickey, B. M.: The Columbia River plume as cross-shelf exporter and along-coast barrier, *Cont. Shelf Res.*, 29, 292–301, <https://doi.org/10.1016/j.csr.2008.03.011>, 2009.
- Banas, N. S., Conway-Cranos, L., Sutherland, D. A., MacCready, P., Kiffney, P., and Plummer, M.: Patterns of river influence and connectivity among subbasins of Puget Sound, with application to bacterial and nutrient loading, *Estuar. Coast.*, 38, 735–753, <https://doi.org/10.1007/s12237-014-9853-y>, 2015.
- Blanke, B. and Raynaud, S.: Kinematics of the Pacific equatorial undercurrent: An Eulerian and Lagrangian approach from GCM results, *J. Phys. Oceanogr.*, 27, 1038–1053, 1997.
- Brasseale, E. and MacCready, P.: The shelf sources of estuarine inflow, *J. Phys. Oceanogr.*, 51, 2407–2421, <https://doi.org/10.1175/JPO-D-20-0080.1>, 2021.
- Brasseale, E., Grason, E. W., McDonald, P. S., Adams, J., and MacCready, P.: Larval transport modeling support for identifying population sources of European green crab in the Salish Sea, *Estuar. Coast.*, 42, 1586–1599, <https://doi.org/10.1007/s12237-019-00586-2>, 2019.
- Brickman, D. and Smith, P. C.: Lagrangian stochastic modeling in coastal oceanography, *J. Atmos. Ocean. Tech.*, 19, 83–99, [https://doi.org/10.1175/1520-0426\(2002\)019<0083:LSMICO>2.0.CO;2](https://doi.org/10.1175/1520-0426(2002)019<0083:LSMICO>2.0.CO;2), 2002.
- Broatch, E. M. and MacCready, P.: Mixing in a Salinity Variance Budget of the Salish Sea is Controlled by River Flow, *J.*

- Phys. Oceanogr., 52, 2305–2323, <https://doi.org/10.1175/JPO-D-21-0227.1>, 2022.
- Burchard, H. and Rennau, H.: Comparative quantification of physically and numerically induced mixing in ocean models, *Ocean Model.*, 20, 293–311, <https://doi.org/10.1016/j.ocemod.2007.10.003>, 2008.
- Chen, C., Limeburner, R., Gao, G., Xu, Q., Qi, J., Xue, P., Lai, Z., Lin, H., Beardsley, R., Owens, B., and Carlson, B.: FVCOM model estimate of the location of Air France 447, *Ocean Dynam.*, 62, 943–952, <https://doi.org/10.1007/s10236-012-0537-5>, 2012.
- Daher, H., Beal, L. M., and Schwarzkopf, F. U.: A new improved estimation of Agulhas leakage using observations and simulations of Lagrangian floats and drifters, *J. Geophys. Res.-Oceans*, 125, e2019JC015753, <https://doi.org/10.1029/2019JC015753>, 2020.
- Dagestad, K.-F., Röhrs, J., Breivik, Ø., and Ådlandsvik, B.: Open-Drift v1.0: a generic framework for trajectory modelling, *Geosci. Model Dev.*, 11, 1405–1420, <https://doi.org/10.5194/gmd-11-1405-2018>, 2018.
- Davis, K. A., Banas, N. S., Giddings, S. N., Siedlecki, S. A., MacCready, P., Lessard, E. J., Kudela, R. M., and Hickey, B. M.: Estuary-enhanced upwelling of marine nutrients fuels coastal productivity in the US Pacific Northwest, *J. Geophys. Res.-Oceans*, 119, 8778–8799, 2014.
- Deltares, D.: Delft3D-FLOW user manual, Deltares Delft, The Netherlands, 330, https://content.oss.deltares.nl/delft3d4/Delft3D-FLOW_User_Manual.pdf (last access: 20 April 2024), 2022.
- Döös, K., Kjellsson, J., and Jönsson, B.: TRACMASS – A Lagrangian trajectory model. In *Preventive methods for coastal protection*, 225–249, Springer, Heidelberg, https://doi.org/10.1007/978-3-319-00440-2_7, 2013.
- Fredj, E., Carlson, D. F., Amitai, Y., Gozolchiani, A., and Gildor, H.: The particle tracking and analysis toolbox (PaTATO) for Matlab, *Limnol. Oceanogr.-Meth.*, 14, 586–599, <https://doi.org/10.1002/lom3.10114>, 2016.
- Garwood, J. C., Fuchs, H. L., Gerbi, G. P., Hunter, E. J., Chant, R. J., and Wilkin, J. L.: Estuarine retention of larvae: Contrasting effects of behavioral responses to turbulence and waves, *Limnol. Oceanogr.*, 67, 992–1005, <https://doi.org/10.1002/lno.12052>, 2022.
- Giddings, S. N., MacCready, P., Hickey, B. M., Banas, N. S., Davis, K. A., Siedlecki, S. A., Trainer, V. L., Kudela, R. M., Pelland, N. A., and Connolly, T. P.: Hindcasts of potential harmful algal bloom transport pathways on the Pacific Northwest coast, *J. Geophys. Res.-Oceans*, 119, 2439–2461, <https://doi.org/10.1002/2013JC009622>, 2014.
- Havens, H., Luther, M. E., and Meyers, S. D.: A coastal prediction system as an event response tool: Particle tracking simulation of an anhydrous ammonia spill in Tampa Bay, *Mar. Pollut. Bull.*, 58, 1202–1209, <https://doi.org/10.1016/j.marpolbul.2009.03.012>, 2009.
- Harris, C. R., Millman, K. J., van der Walt, S. J., Gommers, R., Virtanen, P., Cournapeau, D., Wieser, E., Taylor, J., Berg, S., Smith, N. J., Kern, R., Picus, M., Hoyer, S., van Kerkwijk, M. H., Brett, M., Haldane, A., Fernández del Río, J., Wiebe, M., Peterson, P., Gérard-Marchant, P., Sheppard, K., Reddy, T., Weckesser, W., Abbasi, H., Gohlke, C., and Oliphant, T. E.: Array programming with NumPy, *Nature*, 585, 357–362, <https://doi.org/10.1038/s41586-020-2649-2>, 2020.
- Hoyer, S. and Hamman, J.: xarray: ND labeled arrays and datasets in Python, *J. Open Res. Softw.*, 5, 10, <https://doi.org/10.5334/jors.148>, 2017.
- Hunter, E. J., Fuchs, H. L., Wilkin, J. L., Gerbi, G. P., Chant, R. J., and Garwood, J. C.: ROMSPATH v1.0: offline particle tracking for the Regional Ocean Modeling System (ROMS), *Geosci. Model Dev.*, 15, 4297–4311, <https://doi.org/10.5194/gmd-15-4297-2022>, 2022.
- Jalón-Rojas, I., Wang, X. H., and Fredj, E.: A 3D numerical model to track marine plastic debris (TrackMPD): sensitivity of microplastic trajectories and fates to particle dynamical properties and physical processes, *Mar. Pollut. Bull.*, 141, 256–272, <https://doi.org/10.1016/j.marpolbul.2019.02.052>, 2019.
- Klocker, A. and Abernathey, R.: Global patterns of mesoscale eddy properties and diffusivities, *J. Phys. Oceanogr.*, 44, 1030–1046, <https://doi.org/10.1175/JPO-D-13-0159.1>, 2014.
- Lange, M. and van Sebille, E.: Parcels v0.9: prototyping a Lagrangian ocean analysis framework for the petascale age, *Geosci. Model Dev.*, 10, 4175–4186, <https://doi.org/10.5194/gmd-10-4175-2017>, 2017.
- Lett, C., Verley, P., Mullon, C., Parada, C., Brochier, T., Penven, P., and Blanke, B.: A Lagrangian tool for modelling ichthyoplankton dynamics, *Environ. Model. Softw.*, 23, 1210–1214, <https://doi.org/10.1016/j.envsoft.2008.02.005>, 2008.
- Li, Y., He, R., and Manning, J. P.: Coastal connectivity in the Gulf of Maine in spring and summer of 2004–2009, *Deep Sea Res. Pt. II*, 103, 199–209, <https://doi.org/10.1016/j.dsr2.2013.01.037>, 2014.
- Liang, J. H., Liu, J., Benfield, M., Justic, D., Holstein, D., Liu, B., Hetland, R., Kobashi, D., Dong, C., and Dong, W.: Including the effects of subsurface currents on buoyant particles in Lagrangian particle tracking models: Model development and its application to the study of riverborne plastics over the Louisiana/Texas shelf, *Ocean Model.*, 167, 101879, <https://doi.org/10.1016/j.ocemod.2021.101879>, 2021.
- MacCready, P., McCabe, R. M., Siedlecki, S. A., Lorenz, M., Giddings, S. N., Bos, J., Albertson, S., Banas, N. S., and Garnier, S.: Estuarine circulation, mixing, and residence times in the Salish Sea, *J. Geophys. Res.-Oceans*, 126, e2020JC016738, <https://doi.org/10.1029/2020JC016738>, 2021.
- McKinney, W.: Data structures for statistical computing in python, in: *Proceedings of the 9th Python in Science Conference*, vol. 445, No. 1, 51–56, <https://doi.org/10.25080/Majora-92bf1922-00a>, 2010.
- Melsom, A., Kvile, K. Ø., Dagestad, K. F., Broström, G., and Langangen, Ø.: Exploring drift simulations from ocean circulation experiments: application to cod eggs and larval drift, *Clim. Res.*, 86, 145–162, <https://doi.org/10.3354/cr01652>, 2022.
- Nepstad, R., Nordam, T., Ellingsen, I. H., Eisenhauer, L., Litzler, E., and Kotzakoulakis, K.: Impact of flow field resolution on produced water transport in Lagrangian and Eulerian models, *Mar. Pollut. Bull.*, 182, 113928, <https://doi.org/10.1016/j.marpolbul.2022.113928>, 2022.
- Nordam, T. and Duran, R.: Numerical integrators for Lagrangian oceanography, *Geosci. Model Dev.*, 13, 5935–5957, <https://doi.org/10.5194/gmd-13-5935-2020>, 2020.
- Nordam, T., Nepstad, R., Litzler, E., and Röhrs, J.: On the use of random walk schemes in oil spill modelling, *Mar. Pollut. Bull.*,

- 146, 631–638, <https://doi.org/10.1016/j.marpolbul.2019.07.002>, 2019.
- North, E. W., Hood, R. R., Chao, S. Y., and Sanford, L. P.: Using a random displacement model to simulate turbulent particle motion in a baroclinic frontal zone: A new implementation scheme and model performance tests, *J. Mar. Syst.*, 60, 365–380, <https://doi.org/10.1016/j.jmarsys.2005.08.003>, 2006.
- North, E. W., Schlag, Z., Hood, R. R., Li, M., Zhong, L., Gross, T., and Kennedy, V. S.: Vertical swimming behavior influences the dispersal of simulated oyster larvae in a coupled particle-tracking and hydrodynamic model of Chesapeake Bay, *Mar. Ecol. Progr. Ser.*, 359, 99–115, <https://doi.org/10.3354/meps07317>, 2008.
- North, E. W., Adams, E. E. E., Schlag, Z. Z., Sherwood, C. R., He, R. R., Hyun, K. H. K., Socolofsky, S. A.: Simulating oil droplet dispersal from the Deepwater Horizon spill with a Lagrangian approach, edited by: Liu, Y., Macfadyen, A., Ji, Z.-G., and Weisberg, R. H., in: *Monitoring and Modeling the Deepwater Horizon Oil Spill: A Record-Breaking Enterprise*, 195, 217–226, American Geophysical Union, United States, <https://doi.org/10.1029/2011GM001102>, 2011.
- Onink, V., Jongedijk, C. E., Hoffman, M. J., van Sebille, E., and Laufkötter, C.: Global simulations of marine plastic transport show plastic trapping in coastal zones, *Environ. Res. Lett.*, 16, 064053, <https://doi.org/10.1088/1748-9326/abecbd>, 2021.
- Paris, C. B., Helgers, J., Van Sebille, E., and Srinivasan, A.: Connectivity Modeling System: A probabilistic modeling tool for the multi-scale tracking of biotic and abiotic variability in the ocean, *Environ. Model. Softw.*, 42, 47–54, <https://doi.org/10.1016/j.envsoft.2012.12.006>, 2013.
- Ralston, D. K., Cowles, G. W., Geyer, W. R., and Holleman, R. C.: Turbulent and numerical mixing in a salt wedge estuary: Dependence on grid resolution, bottom roughness, and turbulence closure, *J. Geophys. Res.-Oceans*, 122, 692–712, <https://doi.org/10.1002/2016JC011738>, 2017.
- Ricker, M. and Stanev, E. V.: Circulation of the European north-west shelf: a Lagrangian perspective, *Ocean Sci.*, 16, 637–655, <https://doi.org/10.5194/os-16-637-2020>, 2020.
- Rowe, M. D., Anderson, E. J., Wynne, T. T., Stumpf, R. P., Fanslow, D. L., Kijanka, K., Vanderploeg, H. A., Strickler, J. R., and Davis, T. W.: Vertical distribution of buoyant *Microcystis* blooms in a Lagrangian particle tracking model for short-term forecasts in Lake Erie, *J. Geophys. Res.-Ocean*, 121, 5296–5314, <https://doi.org/10.1002/2016JC011720>, 2016.
- Schlag, Z. R. and North, E. W.: Lagrangian TRANSPORT model (LTRANS v.2) User's Guide, University of Maryland Center for Environmental Science, Horn Point Laboratory, Cambridge, MD, USA, Tech. rep., 183 pp., https://northweb.hpl.umces.edu/LTRANS/LTRANSv2/LTRANSv2_UsersGuide_6Jan12.pdf (last access: 20 April 2024), 2012.
- Shchepetkin, A. F. and McWilliams, J. C.: The regional oceanic modeling system (ROMS): a split-explicit, free-surface, topography-following-coordinate oceanic model, *Ocean Model.*, 9, 347–404, <https://doi.org/10.1016/j.ocemod.2004.08.002>, 2005.
- Siedlecki, S. A., Banas, N. S., Davis, K. A., Giddings, S., Hickey, B. M., MacCready, P., Connolly, T., and Geier, S.: Seasonal and interannual oxygen variability on the Washington and Oregon continental shelves, *J. Geophys. Res.-Oceans*, 120, 608–633, 2015.
- Smolarkiewicz, P. K.: A fully multidimensional positive definite advection transport algorithm with small implicit diffusion, *J. Comput. Phys.*, 54, 325–362, [https://doi.org/10.1016/0021-9991\(84\)90121-9](https://doi.org/10.1016/0021-9991(84)90121-9), 1984.
- Stone, H. B., Banas, N. S., and MacCready, P.: The effect of alongcoast advection on Pacific Northwest shelf and slope water properties in relation to upwelling variability, *J. Geophys. Res.-Oceans*, 123, 265–286, <https://doi.org/10.1002/2017JC013174>, 2018.
- Stone, H. B., Banas, N. S., MacCready, P., Trainer, V. L., Ayres, D. L., and Hunter, M. V.: Assessing a model of Pacific Northwest harmful algal bloom transport as a decision-support tool, *Harmful Algae*, 119, 102334, <https://doi.org/10.1016/j.hal.2022.102334>, 2022.
- Sutherland, D. A., MacCready, P., Banas, N. S., and Smedstad, L. F.: A model study of the Salish Sea estuarine circulation, *J. Phys. Oceanogr.*, 41, 1125–1143, 2011.
- Testa, J. M., Eric Adams, E., North, E. W., and He, R.: Modeling the influence of deep water application of dispersants on the surface expression of oil: A sensitivity study, *J. Geophys. Res.-Oceans*, 121, 5995–6008, <https://doi.org/10.1002/2015JC011571>, 2016.
- Thomson, R. E. and Emery, W. J.: *Data analysis methods in physical oceanography*, Newnes, Elsevier, 3rd edn., 615–616, ISBN 978-0-12-387782-6, 2014.
- van Sebille, E., Griffies, S. M., Abernathey, R., Adams, T. P., Berloff, P., Biastoch, A., Blanke, B., Chassignet, E. P., Cheng, Y., Cotter, C. J., Deleersnijder, E., Döös, K., Drake, H. F., Drijfhout, S., Gary, S. F., Heemink, A. W., Kjellsson, J., Koszalka, I. M., Lange, M., Lique, C., MacGilchrist, G. A., Marsh, R., Mayorga Adame, C. G., McAdam, R., Nencioli, F., Paris, C. B., Piggott, M. D., Polton, J. A., Rühls, S., Shah, S. H. A. M., Thomas, M. D., Wang, J., Wolfram, P. J., Zanna, L., and Zika, J. D.: Lagrangian ocean analysis: Fundamentals and practices, *Ocean Model.*, 121, 49–75, <https://doi.org/10.1016/j.ocemod.2017.11.008>, 2018.
- Vennell, R., Scheel, M., Weppe, S., Knight, B., and Smeaton, M.: Fast lagrangian particle tracking in unstructured ocean model grids, *Ocean Dynam.*, 71, 423–437, <https://doi.org/10.1007/s10236-020-01436-7>, 2021.
- Virtanen, P., Gommers, R., Oliphant, T. E., Haberland, M., Reddy, T., Cournapeau, D., Burovski, E., Peterson, P., Weckesser, W., Bright, J., van der Walt, S. J., Brett, M., Wilson, J., Millman, K. J., Mayorov, N., Nelson, A. R. J., Jones, E., Kern, R., Larson, E., Carey, C. J., Polat, Í, Feng, Y., Moore, E. W., VanderPlas, J., Laxalde, D., Perktold, J., Cimrman, R., Henriksen, I., Quintero, E. A., Harris, C. R., Archibald, A. M., Ribeiro, A. H., Pedregosa, F., van Mulbregt, P., and SciPy 1.0 Contributors: SciPy 1.0: fundamental algorithms for scientific computing in Python, *Nat. Methods*, 17, 261–272, <https://doi.org/10.1038/s41592-019-0686-2>, 2020.
- Visser, A. W.: Using random walk models to simulate the vertical distribution of particles in a turbulent water column, *Mar. Ecol. Progr. Ser.*, 158, 275–281, <https://doi.org/10.3354/meps158275>, 1997.
- Wagner, P., Rühls, S., Schwarzkopf, F. U., Koszalka, I. M., and Biastoch, A.: Can Lagrangian tracking simulate tracer spreading in a high-resolution Ocean General Circulation Model?, *J. Phys. Oceanogr.*, 49, 1141–1157, <https://doi.org/10.1175/JPO-D-18-0152.1>, 2019.

- Wang, S., Zhao, L., Wang, Y., Zhang, H., Li, F., and Zhang, Y.: Distribution characteristics of green tides and its impact on environment in the Yellow Sea, *Mar. Environ. Res.*, 181, 105756, <https://doi.org/10.1016/j.marenvres.2022.105756>, 2022.
- Xiong, J. and MacCready, P.: Model hydrodynamic outputs and example codes for running different Lagrangian particle tracking packages, Zenodo [code], <https://doi.org/10.5281/zenodo.10810102>, 2024.
- Xiong, J., Shen, J., Qin, Q., Tomlinson, M. C., Zhang, Y. J., Cai, X., Fei, Y., Lin, C., and Mulholland, M.: Biophysical interactions control the progression of harmful algal blooms in Chesapeake Bay: A novel Lagrangian particle tracking model with mixotrophic growth and vertical migration, *Limnol. Oceanogr. Lett.*, 8, 498–508, <https://doi.org/10.1002/lol2.10308>, 2023.